SYMMETRIC PARSEC-SCALE OH MEGAMASER STRUCTURES IN ARP 220

COLIN J. LONSDALE
MIT Haystack Observatory, Off Route 40, Westford, MA 01886; cjl@dopey.haystack.edu

CAROL J. LONSDALE
Infrared Processing and Analysis Center, California Institute of Technology, 100-22, Pasadena, CA 91125; cjl@ipac.caltech.edu

PHILIP J. DIAMOND
National Radio Astronomy Observatory, Socorro, NM 87801; pdiamond@nrao.edu

AND

HARDING E. SMITH[1]
Center for Astrophysics and Space Sciences, University of California, San Diego, La Jolla, CA 92093-0424; hsmith@ucsd.edu

ABSTRACT

The parsec-scale OH megamaser emission in the luminous IR galaxy Arp 220 has been imaged in detail using a global VLBI array. Four major emission regions are revealed in the 1667 MHz line, each with complex spatial and velocity structure showing intriguing symmetries. These emission regions have no associated continuum emission to stringent limits, and the brighter components have a maser amplification ratio exceeding 800. No compact emission is detected in the 1665 MHz line. The compact maser emission, with high amplification and unmeasurably small 1665/1667 line ratio, appears to be the result of saturated masers in physically compact masing clouds. The diffuse emission, on the other hand, appears to fit the traditional OH megamaser model of a low-gain masing screen on scales of hundreds of parsecs. Infrared pumping is indicated for the diffuse emission, but collisional pumping is probably important for the compact components. The compact components may trace shock fronts in the dense nuclear environment and may be related to active galactic nucleus activity.

Subject headings: galaxies: active — infrared: galaxies — masers — radio lines: galaxies

1. INTRODUCTION

OH megamasers are found in the nuclear regions of powerful infrared galaxies, exhibiting line luminosities approaching 10^4 $L_\odot$. Arp 220 (IC 4553), at a distance of 76 Mpc, is the prototype OH megamaser galaxy, exhibiting the classical properties of a double-peaked line profile a few hundred km s^{-1} wide, with a high 1667-to-1665 MHz line ratio (Baan, Wood, & Haschick 1982; Henkel & Wilson 1990). Megamasers have been interpreted as being caused by an extended, low-gain molecular screen, distributed over a few hundred parsec region, which amplifies the nuclear radio continuum (Henkel & Wilson 1990; Randell et al. 1995).

Diamond et al. (1989) performed the first VLBI observations of OH megamasers, showing that the OH structure in Arp 220 was concentrated in two regions coinciding with the strong radio continuum emission, consistent with this model. This picture was modified substantially by Lonsdale et al. (1994, hereafter LDSL94), who demonstrated that the masing gas is physically confined to a small volume, presumably deep in the twin nuclei of Arp 220. Because recent studies indicate extreme obscuration by dust and gas in the nuclear regions (see, e.g., Scoville, Yun, & Bryant 1997), such sources are likely to be optically thin only in the radio and hard X-ray spectral regions, and nuclear OH megamasers are therefore a valuable probe of the central energy sites of powerful infrared galaxies.

The small physical extent of the masing clouds revealed by the LDSL94 data posed difficulties for conventional IR pumping schemes involving a cool (60K) extended (300 pc) IR source. The results argued instead for a smaller, warmer pump source, and LDSL94 favored a model involving a nuclear molecular torus surrounding a hidden active galactic nucleus

(AGN). In order to test this model, and to exploit the potential of the OH megamasers as probes of the IR galaxies, we conducted a major new VLBI imaging experiment on the four brightest OH megamasers accessible to a northern VLBI array: Arp 220, III Zw 35, IRAS F17208, and Mrk 231. All except Mrk 231 were imaged in OH. Here we present the main results of our spectral line imaging of Arp 220 at ~1 pc resolution, deferring a detailed analysis of the extensive data set to a future paper. The results for III Zw 35 and IRAS F17208 are discussed by Diamond et al. (1998), the continuum data for Mrk 231 in Lonsdale et al. (1998), and the continuum images of Arp 220 in Smith et al. (1998).

2. OBSERVATIONS AND RESULTS

The observations, conducted under project code GL15 on 1994 November 13, involved 17 telescopes in Europe and the US, and covered three of the four OH maser lines plus the continuum. Arp 220 received a continuous 7 hr track, of which 4.2 hr was spent on-source, yielding excellent *u-v* coverage. The data were correlated on the NRAO VLBA correlator in Socorro, NM, in 1996 April, with a spectral resolution of 15.1625 kHz (2.86 km s^{-1}). The data were analyzed using the AIPS package.

Amplitude calibration was performed using telescope Tsys logs, while phasecal and delay determination was done using data on the calibrators 1300+580 and OQ 208, observed periodically during the run. Complex bandpass calibrations were derived from observations of 3C 84. The fringe rates for Arp 220 were determined by fringe fitting to the line peak, which was clearly visible in the raw data on all baseline lengths. The antenna-based phases were corrected, and the amplitude calibration was refined, using self-calibration at the line peak. All these solutions, for phasecal, delay, rate, bandpass, phase, and

---

[1] Also Infrared Processing and Analysis Center, California Institute of Technology.

amplitude, were transferred uniformly to the rest of the line and continuum data sets.

The data were edited for discrepant points, and imaged using the AIPS IMAGR program. The angular resolution of the images was approximately 3.1 × 8.0 mas (1.0 × 2.5 pc for Arp 220 at an assumed distance of 76 Mpc). The rms noise level on the images was 1.3 mJy beam^{-1} at a spectral resolution of 2.86 km s^{-1} (15.625 kHz), and 0.03 mJy beam^{-1} in the continuum images with 26 MHz bandwidth. We display a small subset of the images here, chosen to best illustrate the principal results of the study. Figures 1 and 2 show the morphology of the compact OH emission in the western and eastern nuclei, respectively, along with component spectra, and velocity profiles across the brightest features. The images presented by Diamond et al. (1989) are broadly consistent with the much higher quality data presented here. The continuum images, which show numerous sub-millijansky unresolved point sources interpreted as highly luminous starburst-related radio supernovae, are presented and discussed in the companion paper by Smith et al. (1998, hereafter SLLD98) and are not shown here, though we frequently refer to these results.

2.1. *Maser Emission Characteristics*

Arp 220 has two nuclei in the radio and near-infrared continuum, separated by about 0″.95 (Condon et al. 1991; Mazzarella et al. 1992). There are four major OH maser regions, two in each of the nuclei. In each nucleus, one of the emission regions has a highly elongated structure, and one has a more amorphous structure with somewhat less compact features. The velocity ranges of the four components overlap each other significantly. In both cases the linear component is to the north, and the amorphous component is to the south. We adopt labels W1, W2, E1, and E2 for the four components, where the first character refers to the appropriate nucleus, "1" refers to the linear northern component, and "2" refers to the amorphous southern component.

Component W1 (see Fig. 1) shows a narrow, smooth, linear ridge of emission about 25 pc long and less than 1 pc wide oriented in position angle ∼150°, with a compact central feature spanning many velocity channels that is spatially unresolved in individual velocity channels. This central feature displays evidence of a marginally resolved, nonlinear transverse velocity gradient. The linear ridge displays a well defined, symmetric velocity gradient of ∼3 km s^{-1} pc^{-1}, with increasing blueshift away from the central feature on both sides (i.e., the ends of the structure are blueshifted, and the center is redshifted).

Component W2 consists of a slightly resolved ridge oriented roughly N-S, with a more diffuse region of emission immediately to the east. The velocity structure is complex. The overall extent of the main component is roughly 15 × 10 pc. About 15 pc to the SW is a barely resolved maser feature ≤2 pc across, which is blueshifted from the main W2 component by ∼100 km s^{-1}. The W2 component is spectrally very broad and is located near the southern edge of a cluster of continuum point sources (SLLD98), none of which are coincident with the strong maser features.

In the eastern nucleus (Fig. 2), component E1 consists of a string of compact maser spots about 30 pc long oriented roughly E-W, which curves smoothly through about 30° along its length. Most of the maser spots have relatively narrow velocity width, of order 20–40 km s^{-1}. One component, however, located at the center of the string of spots, has a very broad velocity width
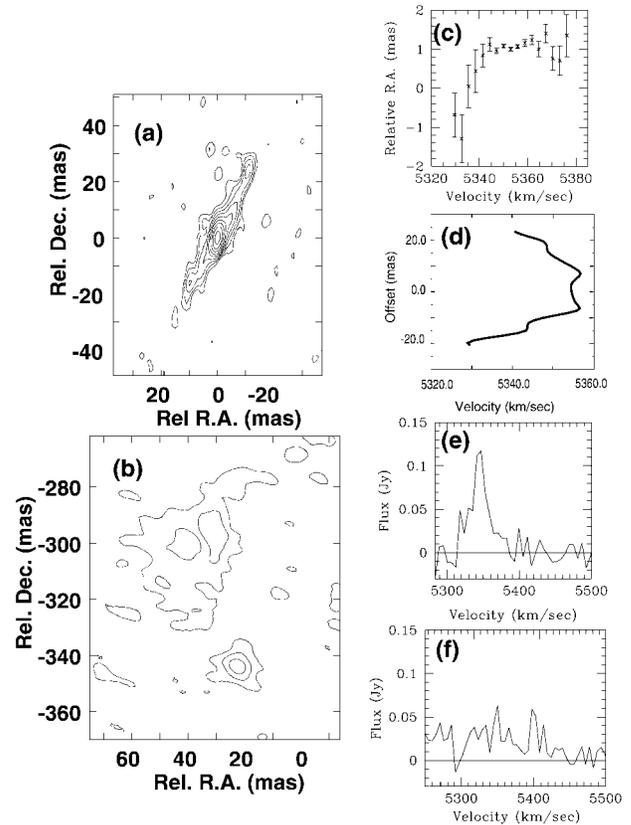

FIG. 1.—The western nucleus of Arp 220 in the 1667 MHz OH line. The angular resolution in (*a*), showing component W1, is 3.1 × 8.0 mas (1.1 × 2.9 pc) in p.a. ∼ 0°. (*b*) Component W2 has been tapered to a resolution of 8 × 8 mas (2.9 × 2.9 pc), owing to poor SNR in the full-resolution image although more compact structures are apparent at full resolution. Contour levels are separated by a factor of $2^{1/2}$. Panel (*a*) is averaged over the velocity range 5300–5400 km s^{-1}, while (*b*) is averaged over 5200–5450 km s^{-1}. (*c*) Transverse velocity profile across the peak of W1. (*d*) Velocity profile along the W1 ridge line. Panels (*e*) and (*f*) show the integrated spectra of W1 and W2, respectively.

of more than 150 km s^{-1}. This component displays a sharp velocity gradient approximately perpendicular to the overall elongation of E1. The individual maser spots are generally barely resolved (source sizes 1–2 pc).

Component E2 is morphologically similar to component W2, with a narrow, barely resolved ridge of emission ∼10 pc long, and more diffuse emission to the west of the ridge. The velocity structure is complex, with an overall SE-to-NW gradient superimposed.

The central features of components W1 and E1 stand out among the compact maser spots in terms of their brightness and broad velocity width. The fact that each of these unusual maser spots accurately bisects the angular extent of the elongated structures containing them constitutes a symmetry property of components W1 and E1 that requires explanation. There is *no evidence* of compact continuum emission above a level of 0.1 mJy coincident with any of the four major emission regions, with a lower limit to the maser amplification factor in the brightest spots of ∼800. In addition to the four main maser components, several weak isolated maser spots are seen, generally confined to the vicinity of one or the other nucleus. These spots are compact and spectrally narrow. Two weak (∼5 mJy), unresolved maser components, positionally coincident with
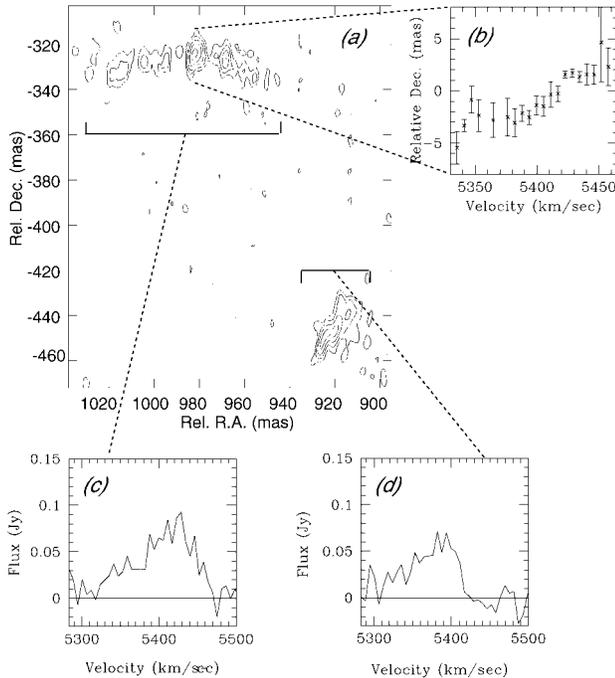
Fig. 2.—The eastern nucleus of Arp 220. (*a*) Image of the eastern nucleus of Arp 220 in the 1667 MHz OH line. The angular resolution and contour levels are the same as those in Fig. 1*a*, and the emission has been averaged over the velocity range 5300–5500 km s^{-1}. (*b*) Transverse velocity gradient across the bright central feature of component E1. Panels (*c*) and (*d*) show the integrated 1667 MHz spectra of components E1 and E2, respectively.

each other but separated by 160 km s^{-1} in velocity, are detected which are aligned with one of the continuum sources (source NW 10 of SLLD98) to ~1 mas.

We are able to account for roughly two-thirds of the total 1667 MHz line luminosity of Arp 220 between 5250 and 5500 km s^{-1}, leaving about one-third to be accounted for by the diffuse maser component. Owing to limited sensitivity, particularly to multiple weak compact sources, the contribution of compact emission to the line wings is less well determined.

We also imaged the source in the 1665 MHz line, anticipating emission at about 20% of the strength of the 1667 MHz emission, in accord with the line ratio from single-dish measurements. Instead, the 1665 MHz emission is conspicuously absent to stringent levels across the entire field of view. For the brightest maser features, the 1667/1665 line ratio exceeds 100, and for all features has only a lower limit. We conclude that all the 1665 MHz emission is diffuse and that the diffuse OH maser emission on scales of 0".1 and greater has an approximately thermal line ratio of 1.8 corresponding to the low-gain limit. We also failed to detect compact 1720 MHz emission from Arp 220, suggesting that this line also arises in the diffuse maser gas.

3. DISCUSSION

3.1. *The Diffuse Maser Component*

Hitherto, the overall properties of OH megamasers have been interpreted in terms of a single maser component, with a particular cloud gain and covering factor (Henkel & Wilson 1990; Randell et al. 1995). The results presented here instead show that the OH masers in Arp 220 are of at least two main types, one diffuse and the other compact, with sharply distinct ob-

servational characteristics. We have shown that the diffuse component shows low amplification (≤ 1) in Arp 220, with an approximately thermal 1667/1665 line ratio. This emission is well explained by a conventional OH megamaser model with relatively low cloud gain, relatively high cloud covering factor, and pumping from the far-IR radiation field. It is this component that is almost certainly related to the OH absorption lines in the mid-IR recently detected by *Infrared Space Observatory* (*ISO*) (Skinner et al. 1997).

The maser spots aligned with the continuum source NW 10 (SLLD98) are clearly associated with the diffuse maser component, and the wide velocity separation of the two spots indicates that the low-gain masing clouds probably occupy a relatively large volume.

3.2. *The Compact Maser Component*

The compact maser component is characterized by high gain, very high 1667/1665 line ratio, high brightness temperature, and a filamentary appearance with very high axial ratios. The observational lower limits on the maser amplification factors range up to 800, set by the limit on positionally coincident continuum emission. However, at least for the peak of W1 it is likely that the true amplification factor is in excess of 10^4. This follows from the fact that the morphology of W1 differs from that of the compact continuum sources detected in Arp 220 (SLLD98) and is thus inconsistent with the amplification of a similar undetected compact continuum source at this position. The diffuse background can supply only a few μJy of continuum emission for maser amplification. Saturation of the compact masers is suggested by the general absence of evidence for amplification of background continuum emission, in conjunction with the high deduced gains, measured brightness temperatures of up to 10^{10} K, and the absence of any detectable time variability. This conclusion differs from that of LDSL94, who were able to measure only a relatively modest lower limit to the amplification.

The observed sizes of the compact masing spots probably correspond closely to the true projected physical sizes of the masing clouds. Most of the individual maser spots in Arp 220 are compact, measuring less than a few parsecs, yet they generally display line widths of several tens of km s^{-1}, compared to natural line widths of much less than 1 km s^{-1}. This sharply reduces the likelihood that the maser spots sample a large masing cloud along a particular velocity-coherent line of sight. We note that the broad velocity width of individual maser spots contributes significantly to the breadth of the integrated OH spectrum of Arp 220, contrary to previous assumptions that large-scale rotational motions in an ensemble of clouds was responsible (see, e.g., Staveley-Smith et al. 1992).

We now address the question of the pumping mechanism for the compact masers. The high frequency of megamasers among LIGs (Sanders et al. 1988; Baan 1989) requires that the maser emission be emitted into a large fraction of 4π steradians. For Arp 220 this implies $L_{OH} \approx 500$ $L_\odot$. Any model for the maser pumping must accommodate such large luminosities. As shown by LDSL94, FIR pumping mechanisms are strongly constrained by geometrical considerations. One can show that the small measured maser sizes require IR pump efficiencies far in excess of the $\leq 1\%$ efficiency thought to prevail (Randell et al. 1995). Contrived geometries cannot alleviate this problem.

Given these problems with infrared pumping, we consider the possibility that the pump may be collisional. The filamen-

tary appearance of W1 and E1 suggests shock fronts, which would heat and compress a molecular medium estimated to have an ambient density exceeding 10^4 cm^{-3} (Scoville et al. 1997), sharply enhancing collision rates with H_2 and perhaps giving rise to the masers. M. Gray (1997, private communication) suggests that predominantly collisional pumping is possible in regions of $n_H \approx 5 \times 10^5 \rightarrow 3 \times 10^6$ and that it might provide the catalyst for maser action to begin and that IR radiation originating in cool (10 K $\rightarrow$ 50 K) dust local to the masers then contributes additional pump power capable of producing the observed maser radiation.

One possible source of shock waves is the starbursting regions delineated by the clusters of continuum sources interpreted as RSN by SLLD98, though W1 is well separated from these regions. The coherence of the maser structures on 20–30 pc scales indicates relatively large-scale disturbances, rather than shocks associated with individual supernovae. The observed systematic velocity gradients in components W1 and E1 may indicate shear across a shock front, possibly associated with the generation of the large scale superwind observed in Arp 220 (Heckman et al. 1996). Nevertheless, there is no ready explanation in this picture for the morphological differences between components 1 and 2 in each nucleus, nor for the central feature symmetry, which is prominent in both W1 and E1.

Another possibility is that the bright, spectrally broad features in the middle of both W1 and E1 arise from collisionally pumped OH in molecular tori orbiting the central masses of two newly formed AGNs. This possibility is supported by a clear transverse velocity gradient in E1 (Fig. 2b), and indications of such a gradient in W1 (Fig. 1c). The mean gradients are of order 50 km s^{-1} pc^{-1}, corresponding to an enclosed mass density of $\sim$1.4 $\times 10^5$ $M_\odot$ pc^{-3}, a total enclosed mass in excess of 10^6 $M_\odot$, and a lower limit to the Eddington luminosity of a few percent of the total bolometric of Arp 220. One might expect AGN central engines to be well fed in such an environment, suggesting that such putative AGNs could be energetically significant. The strikingly symmetrical, elongated features on either side of the central feature might be regions shocked by the passage of twin AGN jets, and the curvature

apparent in E1 could be analogous to the curvature in head-tail radio sources caused by lateral ram pressure due to motion through the ambient medium. The lack of such curvature in W1 may be caused by the plane of curvature falling in the line of sight, a conjecture supported by the striking velocity signature of this component (Fig. 1d). Curvature in a plane containing the line of sight, coupled with some acceleration of the shocked material by the jets would produce the observed velocity structure. However, this model fails to account for components W2 and E2. Large mid-infrared optical depths to the AGN sources could account for the absence of AGN-related high-excitation lines (Sturm et al. 1996). Radio continuum emission from the putative AGNs may be free-free absorbed by the inner torus, or may, as in most AGNs, be intrinsically weak.

We conclude that the OH megamasers in Arp 220 are of two distinct types, one diffuse and the other compact. The diffuse masers are unsaturated, of low gain, and pumped by IR radiation. The compact masers appear to be saturated, collisionally pumped, and probably trace shock fronts in the dense nuclear molecular medium. It is interesting that some OH megamasers have high 1667/1665 MHz line ratios, and display high OH to FIR luminosity ratios, exacerbating IR pumping requirements. We speculate that these systems are dominated by collisionally pumped compact maser components similar to those described here. Much of the broad megamaser line width is intrinsic to the compact maser spots and is not caused by large-scale rotational motions of an ensemble of clouds. The properties of the compact masers in Arp 220 suggest that they may trace newly formed AGN molecular tori and jets. Future higher sensitivity observations should clarify this issue.

REFERENCES

Baan, W. A. 1989, ApJ, 338, 804

Baan, W. A., Wood, P. A. D., & Haschick, A. D. 1982, ApJ, 260, L49

Condon, J. J., Huang, Z.-P., Yin, Q. F., & Thuan, T. X. 1991, ApJ, 378, 65

Diamond, P. J., Lonsdale, C. J., Smith, H. E., & Lonsdale, C. J. 1998, ApJ, submitted

Diamond, P. J., Norris, R. P., Baan, W. A., & Booth, R. S. 1989, ApJ, 340, L49

Heckman, T. M., Dahlem, M., Eales, S. A., Fabbiano, G., & Weaver, K. 1996, ApJ, 457, 616

Henkel, C., & Wilson, T. L. 1990, A&A, 229, 431

Lonsdale, C. J., Diamond, P. J., Smith, H. E., & Lonsdale, C. J. 1994, Nature, 370, 117 (LDSL94)

Lonsdale, C. J., Lonsdale, C. J., Diamond, P. J., & Smith, H. E. 1998, in preparation

Mazzarella, J. M., et al. 1992, AJ, 103, 413

Randell, J., Field, D., Jones, K. N., Yates, J. A., & Gray, M. D. 1995, A&A, 300, 659

Sanders, D., et al. 1988, ApJ, 325, 74

Scoville, N. Z., Yun, M., & Bryant, P. 1997, ApJ, 484, 702

Skinner, C. J., et al. 1997, Nature, 386, 472

Smith, H. E., Lonsdale, C. J., Lonsdale, C. J., & Diamond, P. J. 1998, ApJ, 493, L17 (SLLD98)

Staveley-Smith, L., et al. 1992, MNRAS, 258, 725

Sturm, E., et al. 1996, A&A, 315, L133

ERRATUM

In the Letter "Symmetric Parsec-Scale OH Megamaser Structures in Arp 220" by Colin J. Lonsdale, Carol J. Lonsdale, Philip J. Diamond, and Harding E. Smith (ApJ, 493, L13 [1998]), the order of the names of the authors was permuted and was published incorrectly. The correct order of the authors is Colin J. Lonsdale, Philip J. Diamond, Harding E. Smith, and Carol J. Lonsdale.